

## Production of $\pi^0$ Mesons by $\gamma$ -Rays on Hydrogen\*

A. SILVERMAN AND M. STEARNS†  
*Cornell University, Ithaca, New York*

(Received August 27, 1952)

The production of  $\pi^0$  mesons in the reaction

$$\gamma + p \rightarrow \pi^0 + p$$

is investigated as a function of the incident  $\gamma$ -ray energy in the region from 200 Mev to 300 Mev. For the  $\pi^0$  emitted at approximately  $90^\circ$  laboratory angle, the differential cross section can be represented by

$$(d\sigma_{\pi^0}/d\Omega)_{\pi/2} = C(K-145)^{1.9 \pm 0.4},$$

where  $K$  = energy of incident  $\gamma$ -ray in Mev. The approximate threshold for the reaction is 145 Mev.

The ratio of the cross section at  $60^\circ$  laboratory angle to that at  $90^\circ$  laboratory angle, for  $\gamma$ -rays between 250 Mev and 300 Mev, is  $1.45 \pm 0.25$ .

### INTRODUCTION

THE first observation of the production of  $\pi_0$  mesons by high energy  $\gamma$ -rays was made by Steinberger, Panofsky, and Steller<sup>1,2</sup> at Berkeley. In this experiment they detected the  $\pi^0$  by observing coincidences between the two decay  $\gamma$ -rays. The measurements they made were the coincidence counting rates as a function of the angle between the  $\gamma$ -ray counters for various angles between the beam direction and the plane of the counters. In this way they were able to establish the decay of the  $\pi^0$  into two  $\gamma$ -rays and the cross section for their production, which turned out to be of the same order as the production cross section for charged mesons. It is also possible to obtain some information, by this technique, on the energy of the  $\pi^0$ , since the counting rate as a function of the angle between the two counters depends upon the energy distribution of the  $\pi^0$ 's. They were thus able to construct a rough picture of the production cross section as a function of the primary  $\gamma$ -ray energy. The present experiment was undertaken in an attempt to obtain more directly the information on the excitation function for the production of  $\pi^0$ 's by  $\gamma$ -rays on hydrogen.

The reaction studied was the following:  $\gamma + p = \pi^0 + p'$ , where  $\gamma$  is an incident  $\gamma$ -ray,  $p$  the target proton, and  $p'$  the recoil proton. Since we are dealing with a two-body collision,  $\gamma$ ,  $\pi^0$ , and  $p'$  are coplanar. Thus, assuming the direction of the  $\gamma$ -ray beam known, there are five dynamical variables involved in the collision: the energy of the  $\gamma$ -ray, the energy and angle of the  $\pi^0$ , and the energy and angle of the recoil proton. Since the conservation laws provide three relationships among the five variables, measuring any two completely specifies all of them. In this experiment we choose to measure the energy and angle of the recoil proton.

\* Work supported by contract with the ONR.

† Now at Carnegie Institute of Technology, Pittsburgh, Pennsylvania.

<sup>1</sup> Steinberger, Panofsky, and Steller, Phys. Rev. **78**, 494 (1950).

<sup>2</sup> Steinberger, Panofsky, and Steller, Phys. Rev. **86**, 180 (1952).

### EXPERIMENTAL

#### Experimental Arrangement

The experimental arrangement is shown schematically in Fig. 1. All of the shielding and collimation has been omitted for the sake of clarity. The  $\gamma$ -ray beam is the bremsstrahlung radiation from the 315-Mev Cornell synchrotron. The reaction is observed by detecting coincidences between the recoil protons and one of the decay  $\gamma$ -rays from the  $\pi^0$  meson. The  $\gamma$ -ray counter is a telescope of three stilbene crystals arranged as follows: As seen from the target there is an anticoincidence crystal, converter, and two crystals in coincidence. This is identical with the  $\gamma$ -ray detector described in references 1 and 2. The proton counter is a cylindrical NaI crystal (0.75 in. thick, 1.50 in. in diameter, mounted on a 5819 RCA phototube) in which the protons expend all of their energy. The pulse height is thus a measure of the proton energy. The pulse height was measured in a five-channel analyzer. The electronics was arranged so that the proton pulse height was measured only when a coincidence between the  $\gamma$ -ray and proton counters was registered.

The target used was a 0.23-g/cm<sup>2</sup> slab of polyethylene ( $\text{CH}_2$ )<sub>n</sub>. The carbon background was determined using a carbon target whose stopping power for protons was equal to that of the polyethylene target.

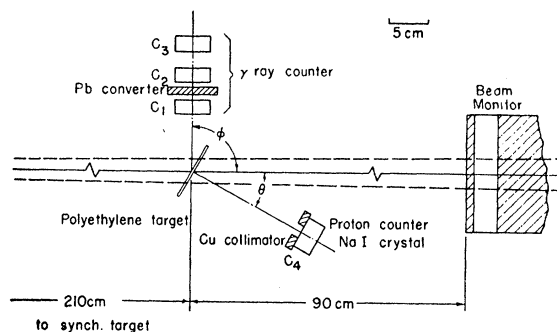


FIG. 1. Experimental arrangement.

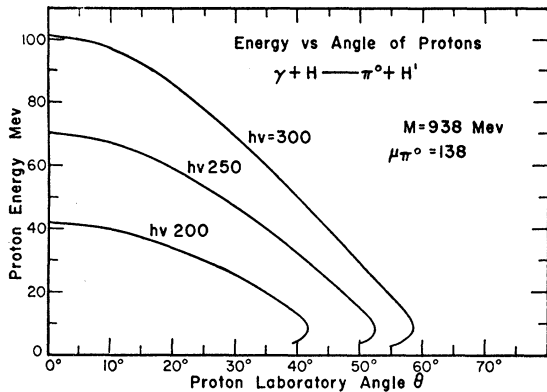


FIG. 2. Recoil proton angle vs proton energy for various  $\gamma$ -ray energies.

### Choice of Angles for the Proton and $\gamma$ -Ray Detectors

Figure 2 shows a graph of the energy of the recoil proton vs laboratory angle for various  $\gamma$ -ray energies. It is seen that the protons are confined to angles less than  $60^\circ$  to the beam direction for all energies up to 315 Mev. In this experiment measurements were made with the proton counter set at  $30^\circ$  and  $45^\circ$  to the beam direction.<sup>3</sup> By observing all protons with energy greater than 20 Mev, we were able to detect protons arising from  $\gamma$ -rays in the interval 200 Mev–315 Mev at  $30^\circ$ , and 250 Mev–315 Mev at  $45^\circ$ . The lower limit of 20 Mev for

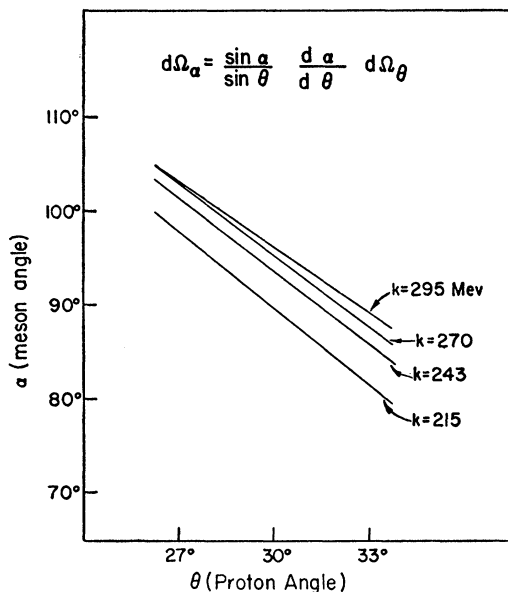


FIG. 3. Relation between the recoil proton angle and the meson angle in the laboratory system for various  $\gamma$ -ray energies

<sup>3</sup> In principle, the technique is useful for measuring the angular distribution of the protons (and hence the  $\pi^0$ 's). In practice, however, difficulties are encountered in the very forward angles because of electron pile up and at angles greater than  $50^\circ$  because here the proton energies become small and the range of  $\gamma$ -ray energies available is reduced (see Fig. 2).

the proton energy was determined primarily by the desire to keep the chance coincidences down to a few percent. There are, however, several other reasons which make it undesirable to decrease this energy substantially. First, the target is about 15 Mev thick so that the resolution becomes bad very rapidly for proton energies below 15 Mev. Second, the double-valued character of the  $E_p$  vs  $\theta$  curve (Fig. 2) make the interpretation ambiguous for low energy proton recoils.

The direction in which the  $\gamma$ -ray counter is placed is dictated by the position of the proton counter. Consider a  $\pi^0$  meson with velocity  $\beta$ . The probability per steradian,  $p(\phi)$ , of one of the decay  $\gamma$ -rays emerging at an angle  $\phi$  with respect of the  $\pi^0$  is

$$p(\phi) = 2(1 - \beta^2) / [4\pi(1 - \beta \cos\phi)^2].$$

This has clearly a maximum for  $\phi = 0$ . Thus, for maximum detection efficiency, the  $\gamma$ -ray detector should be placed in the direction in which the  $\pi^0$  is traveling. In Fig. 3 is

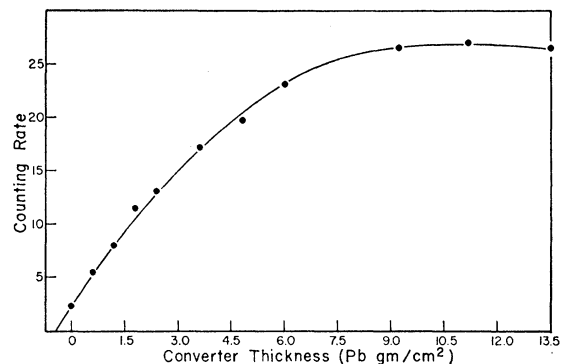


FIG. 4. The curve shows the relative efficiency of the  $\gamma$ -ray counter as a function of converter thickness for 170-Mev  $\gamma$ -rays. The absolute efficiency is obtained by fitting the thin converter data to a curve of form  $1 - e^{-\mu x}$ , where  $\mu$  = absorption coefficient for 170-Mev  $\gamma$ -rays on Pb.

shown the angle of the  $\pi^0$  in the laboratory as a function of the proton laboratory angle for various  $\gamma$ -ray energies. The case shown is for the proton counter set as  $30^\circ$  with an aperture of  $\pm 3^\circ$ . One sees that the  $\pi^0$  angle varies only very slowly with  $\gamma$ -ray energy for a fixed proton angle; and for the proton at  $30^\circ$ , the  $\pi^0$  emerges at close to  $90^\circ$ . With the proton at  $45^\circ$ , the  $\pi^0$  angle is approximately  $60^\circ$  for all  $\gamma$ -ray energies between 250 Mev and 315 Mev.

The energy scale for the proton pulses was determined in a manner similar to that described by Keck.<sup>4</sup> This method consists essentially in measuring the maximum size pulses protons are able to produce in the crystal. These protons have a range just equal to the thickness of the crystal, and consequently their energy can be determined from the range-energy relations. This was checked by observing the photopeak of the ThC'' 2.6-Mev  $\gamma$ -ray. The two results agreed to within ten percent. The calibration provided by the protons was

<sup>4</sup> J. C. Keck, Phys. Rev. **85**, 410 (1952).

used, since it does not involve the large extrapolation from 2.6 Mev to the energy region used in the experiment (20 Mev to 70 Mev).

The efficiency of the  $\gamma$ -ray detector is of considerable importance, particularly for obtaining the absolute cross section. Because of the Doppler shift, the  $\gamma$ -ray energies vary from about 150 Mev to 200 Mev. The variation of the pair production cross section over this energy range is about 5 percent. The efficiency is therefore approximately constant over this region. To get the absolute efficiency, the telescope was calibrated using the 170-Mev  $\gamma$ -ray available at this laboratory.<sup>5,6</sup> Figure 4 shows the counting rate at this energy as a function of converter thickness. Interpolating the results of DeWire *et al.*,<sup>7</sup> we obtain an absorption coefficient of 0.102 cm<sup>2</sup>/g for 170-Mev  $\gamma$ -rays on lead. The converter thickness used was 10 g/cm<sup>2</sup>. From Fig. 4, we calculate the efficiency to be 55 percent. A previous estimate,<sup>8</sup> based on the Monte Carlo calculations of Wilson<sup>9</sup> and related cloud chamber experiments by Shapiro<sup>10</sup> gave a result of 65 percent for the efficiency. The results quoted in the following sections will use the experimental value of 55 percent.

### Auxiliary Experiments

In this section we shall present the results of several auxiliary experiments that were done to check that the coincidences observed were the result of photoproduction of neutral mesons.

(a) Table I shows the relative counting rates for the polyethylene and carbon targets with and without converter. One sees that the carbon background is approximately 20 percent and is independent of converter.<sup>11</sup> The 34 percent residual counting rate with the polyethylene target and no converter is due largely to the carbon background. About  $\frac{1}{3}$  of this rate can be attributed to the efficiency of the  $\gamma$ -ray detector with zero converter since the efficiency with zero converter is about 5 percent due to conversion in the crystals themselves (see Fig. 4).

(b) The maximum proton energy at 30° (Fig. 2), corresponding to 315-Mev  $\gamma$ -rays, is about 72 Mev; and at 45° it is 45 Mev. Furthermore, the maximum backward angle is about 60°. Figure 5 shows the energy distribution of the observed protons at 30°, 45°, and 75°. Histograms A and B have arrows indicating the ex-

TABLE I. Relative counting rates for the poly and carbon targets with and without converter.

Target	Counting rate
Poly	1.00
No target	0.00
Carbon	0.22±0.02
Poly (no converter)	0.34±0.07
Carbon (no converter)	0.24±0.06

pected proton energy for 310-Mev  $\gamma$ -rays at 30° and 45°. It is clear that the maximum proton energy varies as expected as the proton angle is changed. Furthermore, at 75°, an angle forbidden to the recoil proton, the counting rate is zero.

(c) The counting rate was observed with the  $\gamma$ -ray counter rotated 180° about an axis parallel to the beam. The efficiency of the  $\gamma$ -ray counter is then reduced because of two factors: (1) the probability of one of the decay  $\gamma$ -rays striking the detector is reduced by a factor of  $(1-\beta/1+\beta)^2 \cong 1/30$ ; (2) the energy of the  $\gamma$ -ray at 180° to the  $\pi^0$  direction has been greatly reduced. The observed rate was 0.02±0.02 of the initial rate.

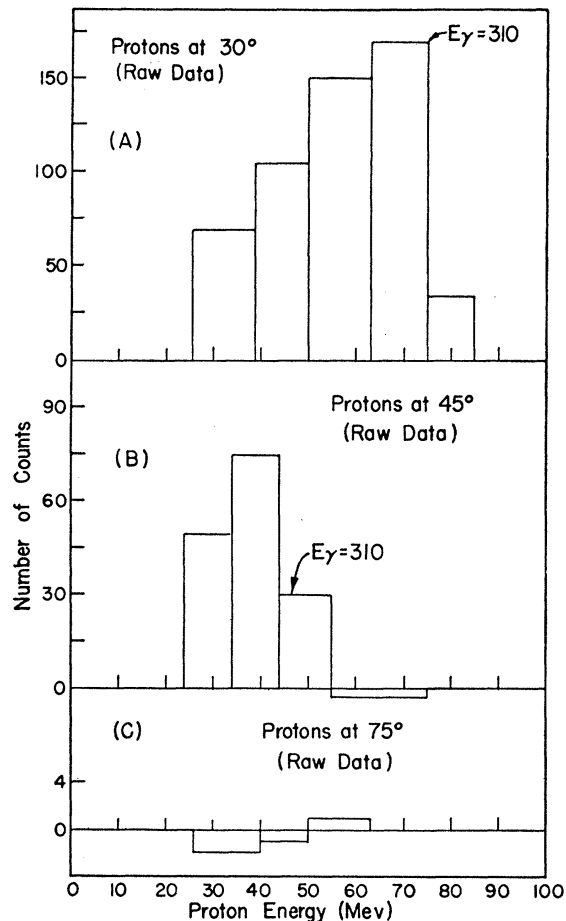


FIG. 5. Histograms showing the number of counts in each energy interval. (A) shows results obtained with the proton counter set at 30°; (B) at 45°; and (C) at 75°.

<sup>5</sup> J. W. Weil and B. D. McDaniel, Phys. Rev. **86**, 582 (1952).

<sup>6</sup> D. Luckey and J. W. Weil, Phys. Rev. **85**, 1060 (1952).

<sup>7</sup> DeWire, Ashkin, and Beach, Phys. Rev. **83**, 505 (1951).

<sup>8</sup> A. Silverman and M. Sterns, Phys. Rev. **83**, 853 (1951).

<sup>9</sup> R. R. Wilson, Phys. Rev. **86**, 261 (1952).

<sup>10</sup> A. Shapiro (private communication).

<sup>11</sup> C. Greifinger and J. Levinger (private communication) have estimated the efficiency per proton in carbon for producing proton-photon coincidences that would be detected by the present apparatus. They take into account (1) the probability that both the  $\pi^0$  and proton escape from nucleus, (2) the effect of initial motion of proton, and (3) the effect of the potential well. They estimate the efficiency to be 5 percent within a factor of 3. The present experiment sets an upper limit of approximately 3 percent for this efficiency. This low efficiency could also be understood quite simply, assuming that several nucleons share the recoil energy.

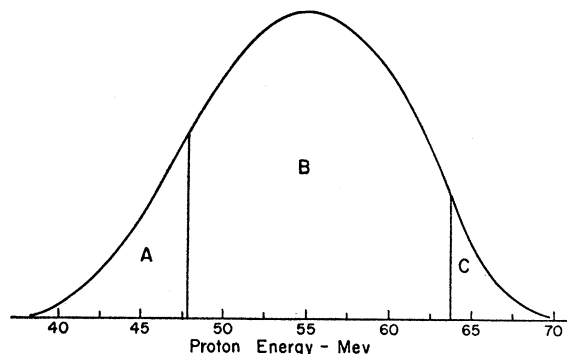


FIG. 6. Resolution curve of the proton counter for 270-Mev  $\gamma$ -rays. See text for discussion of various effects involved in determination of this curve.

(d) Data were taken with a 40-Mev absorber (one that absorbs protons of energy  $\leq 40$  Mev) placed directly in front of the proton counter. The absorber and crystal together were 87 Mev thick. It was found that the energy spectrum shifted downward relative to that measured with no absorber by just the amount expected for protons. This also provided a check on the energy calibration of the proton counter. With the absorber in place, only protons from  $\gamma$ -rays in the region 255–310 Mev were detected. In this interval there were 377 counts with absorber and 354 counts without absorber for equal integrated beams.

To summarize, the results of the experiments described above, provide evidence for the following facts:

(a) Approximately 80 percent of the coincidences are due to the hydrogen content in the polyethylene.

(b) The counts are due to coincidences between  $\gamma$ -rays and protons.<sup>12</sup>

(c) The maximum energy of the protons as a function

TABLE II. Results for the 30° runs.  $K$ = $\gamma$ -ray energy;  $n$ =observed No. of counts;  $n(\text{corr})$  is the No. of counts corrected for "spilling over";  $I(\text{rel})$ =relative No. of  $\gamma$ -rays in the energy interval indicated.

$K$ (Mev)	$K_{Av}$ (Mev)	$n$	$n$ (corr)	$I$ (rel)	$(d\sigma/d\Omega)_{90^\circ}$ cm <sup>2</sup> /steradian
(a) Four-channel analysis (no absorber)					
200–230	215	70	63	1.00	$3.2 \times 10^{-30}$
230–255	243	106	97	0.61	$6.1 \times 10^{-30}$
255–279	267	150	164	0.57	$9.9 \times 10^{-30}$
279–310	295	204	206	0.50	$12.3 \times 10^{-30}$
(b) Three-channel analysis (no absorber)					
200–230	215	70	64	1.00	$3.5 \times 10^{-30}$
230–264	247	151	146	0.95	$6.5 \times 10^{-30}$
264–310	290	309	320	0.85	$12.4 \times 10^{-30}$
(c) Four-channel analysis (no absorber in the two lower energy channels, and 40-Mev Cu absorber in the two higher energy channels)					
200–230	215	67	60	1.00	$2.9 \times 10^{-30}$
230–255	243	103	110	0.65	$6.1 \times 10^{-30}$
255–285	270	200	188	0.70	$8.9 \times 10^{-30}$
285–310	295	177	189	0.39	$14.2 \times 10^{-30}$

<sup>12</sup> These cannot be Compton scattered protons because the angular correlation is wrong.

of the proton angle varies as expected for the reaction  $\gamma + p = \pi^0 + p'$ .

(d) The counting rate as a function of the angle of the  $\gamma$ -ray counter, for fixed proton counter angle, also varies as expected for the above reaction.

## ANALYSIS OF DATA

### Resolving Power of the Proton Detector

The resolving power of the apparatus is determined by three principal features. That is, given a monochromatic  $\gamma$ -ray beam, there are three factors which contribute to the spread in the energy measured for the recoil proton. They are (a) the angular resolution of the proton counter (by far the most important cause of spread), (b) the target thickness, and (c) the resolution of the NaI crystal. The first effect was calculated taking into account the angular aperture of the proton counter and the finite size of the beam. The resolution of the NaI counter was estimated in two ways. First, from the curvature in the high energy tail of the integral number-bias curve taken during the calibration and, second, from the photopeak of the 2.6-Mev ThC''  $\gamma$ -ray. The result was approximately 15 percent width at half-maximum. The results are not sensitive to this number since its effect is not large. The net resolving power of the proton counter was obtained from the fold of these three effects. Figure 6 shows the resolution curve for a 270 Mev  $\gamma$ -ray. The angular aperture of the proton counter in all cases was  $\pm 3^\circ$ . One sees that the resolution curve is quite broad. The major contribution to the width, as previously mentioned, is due to the angular aperture, but because the counting rate is sufficiently small (about one count per minute) it is undesirable to reduce the aperture much. The broadness of the resolution curve limits the fineness with which one can divide the spectrum. For all the analysis the spectrum was divided into three or four intervals. The areas marked B in Fig. 6 shows the limits of the third interval for a four-channel division of the spectrum. It is clear that some of the counts "spill over" into the second interval (A) and the fourth interval (C). In the calculation of the cross sections, the "spilling over" was corrected for.

### Calculation of the Differential Cross Sections

The formula used for the calculation of the differential cross section is

$$\frac{d\sigma}{d\Omega_{\pi^0} dK} = \frac{1}{PNI} \frac{\Delta n}{\Delta\Omega_{\pi^0}}$$

where  $P$ =probability of detecting one of the  $\gamma$ -rays,  $N$ =number of hydrogen atoms per cm<sup>2</sup>,  $I$ =number of incident  $\gamma$ -rays with energy between  $K$  and  $K+dK$ , and  $\Delta n$ =number of counts observed in this interval.

The solid angle  $d\Omega_{\pi^0}$  is the meson solid angle. This can be calculated from the known solid angle subtended by the proton counter.

The probability  $P$  for detecting one of the  $\gamma$ -rays is given by

$$P = \frac{2(1 - \beta_{\pi^0}^2)\epsilon}{4\pi(1 - \beta_{\pi^0} \cos\phi)^2} d\Omega_{\gamma},$$

where  $\beta_{\pi^0}$  = velocity of the  $\pi^0$ ,  $\phi$  = angle between direction of  $\gamma$ -ray counter and velocity vector of the  $\pi^0$ ,  $d\Omega_{\gamma}$  = the solid angle subtended by the  $\gamma$ -ray counter, and  $\epsilon$  = the efficiency of detecting the  $\gamma$ -ray which was measured to be 0.55. (See section on experimental arrangement.)

The number of  $\gamma$ -rays per unit energy interval  $I$  is different than a pure bremsstrahlung spectrum for two reasons: (a) the energy loss in the internal target (40-mil wolfram), and (b) the synchrotron beam is spread out over 2.5 milliseconds. Rather than try to calculate the effect of these corrections, the spectrum was measured with a pair spectrometer<sup>7</sup> under the conditions actually used. The spectrum differed from the bremsstrahlung spectrum primarily at the upper end where the beam spread has its maximum effect.

### RESULTS

The results for the 30° runs are shown in Table II. The column headings are as follows:  $K$  = energy of  $\gamma$ -ray;  $n$  = observed number of counts;  $n(\text{corr})$  is number of counts corrected for the "spilling over" from one channel into another because of the finite resolution;  $I(\text{rel})$  = relative number of  $\gamma$ -rays in the energy interval indicated. Table II(a) is a four-channel analysis of the data taken with no absorber. Table II(b) is a three-channel analysis of the same data. Table II(c) is a mixture of these same data and data taken with the 40-Mev Cu absorber which could only be taken for incident  $\gamma$ -ray energies greater than 255 Mev. The Cu absorber data appear exclusively in the two higher energy channels of Table II(c), while the two lower energy channels use the same raw data used in Table II(a), normalized, however, to the number of monitor readings taken with the Cu absorber and to slightly different channel widths. The differential cross sections for neutral meson production at  $95^\circ \pm 10^\circ$  in the laboratory system are plotted in Fig. 7. The indicated errors are estimated instrumental errors as well as statistical errors. The high energy point is most uncertain because it involves the spectrum of the beam at the end point and the precise upper limit to the beam energy. The absolute cross section is estimated to have an error of about 30 percent arising primarily from uncertainties in measuring the integrated beam and in measuring the efficiency of the  $\gamma$ -ray detector. Figure 8 shows the log of the cross section vs the log of the energy above threshold (145 Mev) for the combined absorber and no absorber data.

Fitting the data with a straight line, one finds a slope equal to 1.9 as determined by a least squares calculation.

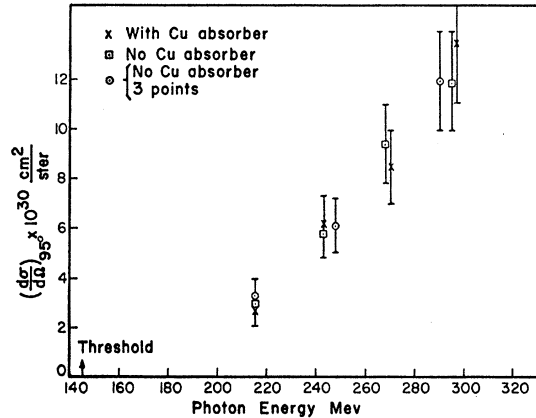


FIG. 7. Differential cross section for  $\pi^0$  production vs photon energy.

Thus, the cross section can be written as

$$(d\sigma_{\pi^0}/d\Omega)_{95^\circ} = C(K - 145)^{1.9 \pm 0.4},$$

where  $K$  = energy of the incident  $\gamma$ -ray.

The data taken with the proton counter at  $45^\circ$  involved  $\gamma$ -rays in the energy interval 255 Mev to 310 Mev. No attempt was made to obtain an excitation function in this region since at most one could obtain only two points. It is clear from the raw data [Fig. 5(b)] that the results are qualitatively similar to that at  $30^\circ$  for the same  $\gamma$ -ray interval. The ratio of the average cross section for  $\gamma$ -rays in the relevant

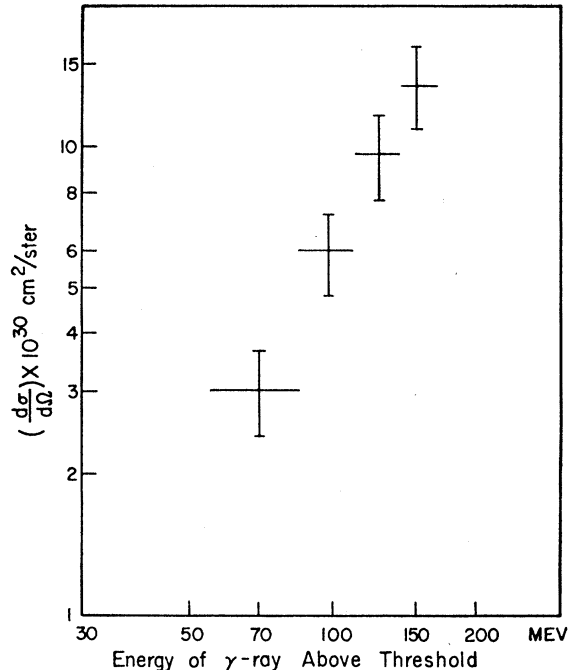


FIG. 8. Log of differential cross section for  $\pi^0$  production vs log of photon energy. Assuming a straight line fit to the data, the slope of the line is  $1.9 \pm 0.4$  as determined by a least squares calculation.

interval has been calculated. The corresponding meson angles in the laboratory system are  $95^\circ$  and  $60^\circ$ . The ratio of the cross sections at these two angles are

$$\frac{(d\sigma/d\Omega_{\pi^0})_{60^\circ}}{(d\sigma/d\Omega_{\pi^0})_{95^\circ}} = 1.45 \pm 0.25.$$

The corresponding ratio and angles in the center-of-mass system are

$$\frac{(d\sigma/d\Omega_{\pi^0})_{75^\circ}}{(d\sigma/d\Omega_{\pi^0})_{110^\circ}} = 1.0 \pm 0.2.$$

The results of the excitation function and the absolute cross sections are in reasonable agreement with the results of Panofsky, Steinberger, and Steller.<sup>2</sup> They do not quote results on the angular distribution for a hydrogen target so that no comparison can be made.

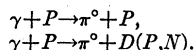
The authors wish to express their gratitude to Professor J. W. DeWire for measuring the spectrum of the spread out beam, to Professor B. D. McDaniel for his assistance in measuring the efficiency of the  $\gamma$ -ray counter, and finally to Professor R. R. Wilson for his continued interest and guidance throughout the course of the experiment.

## Production of $\pi^0$ Mesons in Hydrogen and Deuterium by High Energy $\gamma$ -Rays\*

G. COCCONI AND A. SILVERMAN  
Cornell University, Ithaca, New York

(Received August 27, 1952)

The angular distribution of the  $\pi^0$ 's and the dependence of the cross sections on the energy of the  $\gamma$ -rays have been studied for the reactions



For the first reaction, the angular distribution in the center-of-mass system has the form  $a + b \sin^2 \bar{\theta}$ , with  $a/b \simeq 1$ , and the cross section is proportional to approximately the square of the excess energy of the  $\gamma$ -rays above the threshold;  $\sigma_D/\sigma_H \simeq 2$  at all energies and angles.

### INTRODUCTION

PREVIOUS investigations of  $\pi^0$  production by  $\gamma$ -rays have used detection techniques involving coincidence measurements between two of the products of the reaction, i.e., coincidences either between the two decay  $\gamma$ -rays<sup>1</sup> or between one of the decay  $\gamma$ -rays and the recoiling nucleon.<sup>2</sup> The difficulties involved in the latter technique for angular distribution measurements have been discussed in the preceding paper. The measurement of coincidences between the two decay  $\gamma$ -rays offers certain advantages for angular distribution measurements, but it has the rather serious disadvantage that the counting rates are quite small. As a consequence, the measurements on hydrogen and deuterium, particularly using the usual subtraction technique, become difficult to do with any reasonable statistical accuracy. We have, consequently, been led to investigate the production of  $\pi^0$  mesons on hydrogen and deuterium by detecting only one of the decay  $\gamma$ -rays and thus increasing the counting rates by approximately a factor of 50 over the rates obtained by detecting both  $\gamma$ -rays in coincidence. The increased counting rate is purchased at the cost of some loss in angular definition,

since the decay  $\gamma$ -ray does not necessarily preserve the direction of the  $\pi^0$ . However, this disadvantage turns out to be not too serious because, as shown later, the  $\gamma$ -ray angular distribution reproduces quite faithfully the  $\pi^0$  distribution for the energies with which we are concerned.

### APPARATUS

The experimental arrangement is shown in Fig. 1. The targets used were of cylindrical shape, 2 in. in diameter, 2 in. long, and made of  $H_2O$ ,  $D_2O$ ,  $(CH_2)_n$ , and C. The results for H and D were obtained with the subtraction method. The measurements consisted in recording the coincidences  $(B+C-A)$  between crystals  $B$  and  $C$  with crystal  $A$  in anticoincidence (hereafter called threefold coincidences) and coincidences  $(B+C+D-A)$  between crystals  $B$ ,  $C$ , and  $D$  again with crystal  $A$  in anticoincidence (hereafter called fourfold coincidences) at various angles  $\theta$  and for various maximum energies of the bremsstrahlung  $\gamma$ -ray beam of the Cornell synchrotron. An aluminum absorber  $2\frac{1}{4}$  in. thick was placed between the third and fourth crystal in order to make the fourfold coincidences insensitive to low energy  $\gamma$ -rays. The efficiencies of the threefold and fourfold coincidences as a function of  $\gamma$ -ray energy for a Pb converter 7 g/cm<sup>2</sup> thick are shown in Fig. 2. They were measured for  $\gamma$ -ray energies of 190, 140, and 100

\* This work was supported in part by the ONR.

<sup>1</sup> Panofsky, Steinberger, and Steller, Phys. Rev. **86**, 180 (1952).

<sup>2</sup> A. Silverman and M. Stearns, preceding paper [Phys. Rev. **88**, 1225 (1952)].